J|A|C|S
COMMUNICATIONS

Published on Web 04/27/2004

Characterization of β-Amino Ester Enolates as Hexamers via ^{6}Li NMR Spectroscopy

Anne J. McNeil,[†] Gilman E. S. Toombes,[‡] Sithamalli V. Chandramouli,[§] Benoit J. Vanasse,[§] Timothy A. Ayers,[§] Michael K. O'Brien,[§] Emil Lobkovsky,[†] Sol M. Gruner,[‡] John A. Marohn,[†] and David B. Collum*[,†]

Department of Chemistry and Chemical Biology, Baker Laboratory, Cornell University, Ithaca, New York 14853-1301, Physics Department, Clark Hall, Cornell University, Ithaca, New York 14853-2501, and Aventis, Process Development Chemistry, Bridgewater, New Jersey 08807

Received February 11, 2004; E-mail: dbc6@cornell.edu

As part of a program to prepare new antithrombotic agents, we discovered that unprotected β-amino esters can be exclusively C-alkylated. We sought to optimize this process by studying the structures and reactivities of β-amino ester enolates.[1] Determining the aggregation state of an enolate, however, is especially difficult due to the high symmetry of the possible aggregates—monomers, dimers, tetramers, and hexamers—and the spectroscopically opaque Li−O linkage.[2] Herein we describe a spectroscopic method used to assign β-amino ester enolates (**1**) as hexamers in solution.

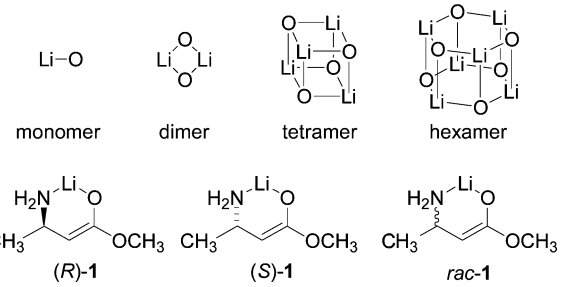

To understand these studies we must briefly digress by describing the dynamic phenomena that are commonly observed for organolithium aggregates but may seem surprising to the nonspecialist.[3] At the lowest attainable NMR probe temperatures (<−100 °C), fast processes including solvent exchange,[4] conformational equilibria,[5] and chelate isomerizations[6] can become observable on NMR spectroscopic time scales, with concomitant spectral complexity. The spectra typically simplify on warming above −100 °C due to time averaging. Further warming of the probe often leads to a particularly odd effect in which *intra*-aggregate exchanges of ^{6}Li nuclei become fast, whereas *inter*-aggregate exchanges are still slow.[7] Consequently, aggregates that differ by virtue of their aggregation numbers (dimers versus hexamers) or subunit composition (4:2 versus 3:3 mixed hexamers) appear as separate species by ^{6}Li NMR spectroscopy, but *each aggregate manifests a single ^{6}Li resonance.* This combination of rapid *intra*-aggregate exchange in conjunction with slow *inter*-aggregate exchange proves critical to the structural assignments.

The ^{6}Li NMR spectrum recorded on [^{6}Li](*R*)-**1** in 9.0 M THF/toluene at −100 °C shows a single resonance, consistent with almost any aggregation state of high symmetry. The ^{6}Li NMR spectrum recorded on [^{6}Li]*rac*-**1** affords a single resonance at a markedly different chemical shift than [^{6}Li](*R*)-**1**, suggesting the formation of a highly symmetric *heterochiral* aggregate. Partially racemic mixtures using combinations of [^{6}Li](*R*)-**1** and [^{6}Li](*S*)-**1** at −100 °C (Figure 1A) show both resonances along with considerable "noise" in the baseline. Additionally, ^{6}Li spectra recorded on [^{6}Li,^{15}N](*S*)-**1** and [^{6}Li,^{15}N]*rac*-**1** show ^{6}Li−^{15}N coupling (d, J_{Li-N} = 3.4 and 3.6 Hz, respectively), confirming chelation as drawn.[8]

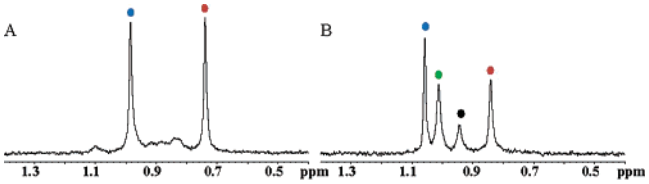

Figure 1. ^{6}Li NMR spectra recorded on a 0.2 M enolate mixture (50% ee) in 9.0 M THF/toluene at (A) −100 °C and (B) −50 °C: (blue) $\mathbf{R_3S_3}$; (green) $\mathbf{R_2S_4}$/$\mathbf{R_4S_2}$; (black) $\mathbf{R_1S_5}$/$\mathbf{R_5S_1}$; (red) $\mathbf{R_6}$/$\mathbf{S_6}$.

Varying the probe temperature from −100 to −50 °C afforded a single sharp resonance for [^{6}Li](*R*)-**1**, offering no evidence of latent stereoisomerism, lower symmetry, or related structural complexity. Conversely, warming samples containing varying proportions of [^{6}Li](*R*)-**1** and [^{6}Li](*S*)-**1** revealed *two* resonances in lieu of the baseline noise—*four* resonances in total (Figure 1B). The data are consistent with deep-seated structural complexities that simplify by rapid *intra*-aggregate exchange at elevated temperatures. Furthermore, the relative intensities are independent of the enolate concentration (0.04−0.40 M) and the THF concentration (2.0−9.0 M), indicating that the four species are at the same aggregation and solvation state.

We considered models based on homochiral aggregates ($\mathbf{R}_N$ or $\mathbf{S}_N$) and heterochiral aggregates ($\mathbf{R}_n\mathbf{S}_{N-n}$). $\mathbf{R}_n\mathbf{S}_{N-n}$/$\mathbf{R}_{N-n}\mathbf{S}_n$ and $\mathbf{R}_N$/$\mathbf{S}_N$ refer to pairs of spectroscopically indistinguishable enantiomers. Dimers ($\mathbf{R_1S_1}$ and $\mathbf{R_2}$/$\mathbf{S_2}$) and tetramers ($\mathbf{R_4}$/$\mathbf{S_4}$, $\mathbf{R_1S_3}$/$\mathbf{R_3S_1}$, and $\mathbf{R_2S_2}$) afford only two and three ^{6}Li resonances, respectively. Conversely, four discrete resonances are consistent with an ensemble of homo- and heterochiral hexamers: $\mathbf{R_6}$/$\mathbf{S_6}$, $\mathbf{R_1S_5}$/$\mathbf{R_5S_1}$, $\mathbf{R_2S_4}$/$\mathbf{R_4S_2}$, and $\mathbf{R_3S_3}$.

A compelling picture emerges from a variant of a Job plot (Figure 2) in which the intensities of the four resonances are plotted as a function of the mole fraction of subunit (*R*)-**1**, X_R.[9] The maximum observed for each aggregate coincides with the stoichiometry of the aggregate. The concentration dependencies were modeled as follows.[10,11]

$$X_R = \frac{\sum_{n=0}^{N} n[\mathbf{R}_n\mathbf{S}_{N-n}]}{\sum_{n=0}^{N} N[\mathbf{R}_n\mathbf{S}_{N-n}]} \qquad X_n = \frac{[\mathbf{R}_n\mathbf{S}_{N-n}]}{\sum_{j=0}^{N} [\mathbf{R}_j\mathbf{S}_{N-j}]}$$

[†] Department of Chemistry and Chemical Biology, Cornell University.
[‡] Physics Department, Cornell University.
[§] Aventis.

10.1021/ja049245s CCC: $27.50

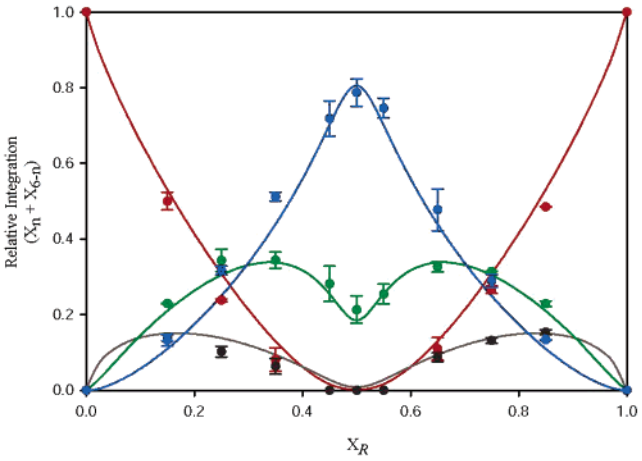

Figure 2. Job plot of the mole fraction of $\mathbf{R}_n\mathbf{S}_{6-n}/\mathbf{R}_{6-n}\mathbf{S}_n$ ($X_n + X_{6-n}$) as a function of the mole fraction of the *R* enantiomer (X_R) at −50 °C. For the case where $n = 3$, only X_3 is plotted. The best fit to the data is also shown: (blue) $\mathbf{R_3S_3}$; (green) $\mathbf{R_2S_4}/\mathbf{R_4S_2}$; (black) $\mathbf{R_1S_5}/\mathbf{R_5S_1}$; (red) $\mathbf{R_6}/\mathbf{S_6}$.

$$[\mathbf{R}_n\mathbf{S}_{N-n}] = C\,\frac{N!}{n!(N-n)!}\,\phi_n \exp\left(\frac{n\mu_R + (N-n)\mu_S}{kT}\right)$$

where

$$\phi_n = \phi_{N-n} = \left\langle \exp\left(\frac{-g_P}{kT}\right)\right\rangle$$

X_n, the mole fraction of the aggregate, is an implicit function of X_R and ϕ_n and may be solved by an iterative parametric method. It is instructive to present the results in terms of the following equilibria:

$$\mathbf{R_3S_3} \overset{K_1}{\rightleftharpoons} {}^1/_2\mathbf{R_6} + {}^1/_2\mathbf{S_6} \quad K_1 = \frac{\phi_0}{20\phi_3}$$

$$\mathbf{R_3S_3} \overset{K_2}{\rightleftharpoons} {}^1/_2\mathbf{R_5S_1} + {}^1/_2\mathbf{R_1S_5} \quad K_2 = \frac{3\phi_1}{10\phi_3}$$

$$\mathbf{R_3S_3} \overset{K_3}{\rightleftharpoons} {}^1/_2\mathbf{R_4S_2} + {}^1/_2\mathbf{R_2S_4} \quad K_3 = \frac{3\phi_2}{4\phi_3}$$

If the aggregate distribution is purely statistical ($\phi_0 = \phi_1 = \ldots = \phi_6$), then $K_1 = 0.05$, $K_2 = 0.30$, and $K_3 = 0.75$. Least-squares fits illustrated in Figure 2 yield substantially different values: $K_1 = 1.0 \pm 0.1 \times 10^{-3}$, $K_2 = 5.0 \pm 0.3 \times 10^{-3}$, and $K_3 = 115 \pm 3 \times 10^{-3}$. From the relationship $\Delta G_m = -RT \ln(K_m/K_{\text{statistical}})$, we obtain the deviations from statistical as follows: $\Delta G_1 = 1.73 \pm 0.04$ kcal/mol, $\Delta G_2 = 1.82 \pm 0.03$ kcal/mol, and $\Delta G_3 = 0.83 \pm 0.01$ kcal/mol. Therefore, the heterochiral $\mathbf{R_3S_3}$ hexamer is markedly more stable than the alternative homo- and heterochiral combinations.

An X-ray crystal structure was obtained of *rac*-**1** showing a prismatic hexamer ($\mathbf{R_3S_3}$) of S_6 symmetry (Figure 3).[12,13] Consistent with the spectroscopic studies, this aggregate would show a single ^{6}Li resonance. The crystallization of the $\mathbf{R_3S_3}$ form is satisfying in light of its relative stability in solution. The high stability of the $\mathbf{R_3S_3}$ hexamer could influence the stereochemistry of alkylation via an asymmetric amplification.[14]

Detailed mechanistic studies on the alkylation of the β-amino ester enolates will be reported in due course. The spectroscopic strategy described herein may prove general for assigning structures of enolates and alkoxides. Last, we are reminded to be cautious about dismissing baseline noise.

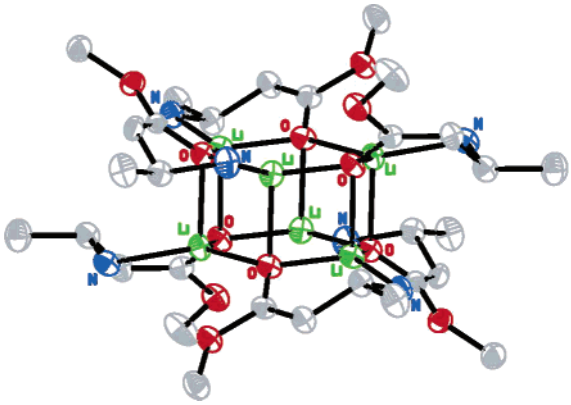

Figure 3. ORTEP of *rac*-**1** revealing a hexameric aggregate of S_6 symmetry. Hydrogen atoms are omitted for clarity.

Acknowledgment. We thank Prof. Benjamin Widom for helpful discussions. A.J.M. and D.B.C. thank the National Institutes of Health for direct support of this work. G.E.S.T. and S.M.G. thank the DOE for support (DE-FG02-97ER62443).

Supporting Information Available: Experimental details, spectroscopic data, mathematical derivations (PDF), and X-ray crystallographic data (CIF). This material is available free of charge via the Internet at http://pubs.acs.org.

References

(1) Enolization was effected without N-lithiation using LiHMDS. Chandramouli, S. V.; O'Brien, M. K.; Powner, T. H. WO Patent 0040547, 2000. See also: Czekaj, M.; Klein, S. I.; Guertin, K. R.; Gardner, C. J.; Zulli, A. L.; Pauls, H. W.; Spada, A. P.; Cheney, D. L.; Brown, K. D.; Colussi, D. J.; Chu, V.; Leadley, R. J.; Dunwiddie, C. T. *Bioorg. Med. Chem. Lett.* **2002**, *12*, 1667−1670. Nagula, G.; Huber, V. J.; Lum, C.; Goodman, B. A. *Org. Lett.* **2000**, *2*, 3527−3529. Myers, A. G.; Gleason, J. L.; Yoon, T. *J. Am. Chem. Soc.* **1995**, *117*, 8488−8489.

(2) Solution studies of enolate aggregation: (a) Wang, D. Z.; Streitwieser, A. *J. Org. Chem.* **2003**, *68*, 8936−8942 and references therein. (b) Jackman, L. M.; Bortiatynski, J. *Adv. Carbanion Chem.* **1992**, *1*, 45−87.

(3) For reviews on Li NMR spectroscopy, see: Günther, H. *J. Braz. Chem.* **1999**, *10*, 241−262. Günther, H. In *Advanced Applications of NMR to Organometallic Chemistry*; Gielen, M., Willem, R., Wrackmeyer, B., Eds.; Wiley & Sons: New York, 1996; pp 247−290.

(4) For leading references, see: Lucht, B. L.; Collum, D. B. *Acc. Chem. Res.* **1999**, *32*, 1035−1042.

(5) Remenar, J. F.; Lucht, B. L.; Kruglyak, D.; Romesberg, F. E.; Gilchirst, J. H.; Collum, D. B. *J. Org. Chem.* **1997**, *62*, 5748−5754. Collum, D. B. *Acc. Chem. Res.* **1993**, *26*, 227−234. Boche, G.; Fraenkel, G.; Cabral, J.; Harms, K.; van Eikema Hommes, N. J. R.; Lohrenz, J.; Marsch, M.; Schleyer, P. v. R. *J. Am. Chem. Soc.* **1992**, *114*, 1562−1565.

(6) (a) Reich, H. J.; Goldenberg, W. S.; Sanders, A. W.; Jantzi, K. L.; Tzschucke, C. C. *J. Am. Chem. Soc.* **2003**, *125*, 3509−3521 and references therein. (b) Aubrecht, K. B.; Lucht, B. L.; Collum, D. B. *Organometallics* **1999**, *18*, 2981−2987.

(7) Bauer, W.; Griesinger, C. *J. Am. Chem. Soc.* **1993**, *115*, 10871−10882. See also ref 6b.

(8) [^{15}N](*S*)-**1** and [^{15}N]*rac*-**1** were synthesized via the Arndt−Eistert homologation: Podlech, J.; Seebach, D. *Liebigs Ann.* **1995**, 1217−1228.

(9) Job, P. *Ann. Chim.* **1928**, *9*, 113−203. Gil, V. M. S.; Oliveira, N. C. *J. Chem. Educ.* **1990**, *67*, 473−478.

(10) Widom, B. *Statistical Mechanics: A Concise Introduction for Chemists*; Cambridge University Press: New York, 2002.

(11) Where μ_R and μ_S are the chemical potentials of *R* and *S*, g_P corresponds to the free energy of assembly for each permutation, and *C* is a constant.

(12) *rac*-**1** (0.20 M) was crystallized from a 9.0 M THF/toluene solution held at −20 °C over 24 h.

(13) For more examples of ester enolate crystal structures, see: Williard, P. G. *Comprehensive Organic Synthesis*; Pergamon: New York, 1991; Vol. 1, pp 1−47. Seebach, D. *Angew Chem., Int. Ed. Engl.* **1988**, *27*, 1624−1654. Boche, G.; Langlotz, I.; Marsch, M.; Harms, K. *Chem. Ber.* **1994**, *127*, 2059−2064. Jastrzebski, J. T. B. H.; van Koten, G.; van de Mieroop, W. F. *Inorg. Chim. Acta* **1988**, *142*, 169−171.

(14) Fenwick, D. R.; Kagan, H. B. *Top. Stereochem.* **1999**, *22*, 257−296.

JA049245S